OTSK1A

Atmospheric Correction for Ocean Color

A. Algorithm Outline

(1) Algorithm name: Atmospheric Correction for Ocean Color

(2) Product Code: NWLR

(3) PI names: G-0065 Hajime Fukushima

(4) Overview of the algorithm (Status: Operational level)

This algorithm is an extension of the OCTS atmospheric correction algorithm (Fukushima et al., 1998). It treated multiple scattering among the aerosol particles and gas molecules, as well as the effects of variable ozone concentration, surface pressure, surface wind speed, and water vapor amount. The atmospheric correction with iterative procedure was developed to avoid the black pixel assumption, and to consider absorptive aerosol. Due to saturation problems of the GLI nominal band16 (749nm) and band18 (865nm), alternative bands (band13:678nm and band19:865nm) are used to estimate base aerosol type. In addition, 380nm and 865nm bands are used to estimate aerosol absorption. In the iteration, the water reflectance at near infrared and 380nm bands are estimated by an in-water model for chlorophyll a (chl) and inorganic suspended matter (ism) concentrations as well as absorption coefficient of colored dissolved organic matter (cdom). These parameter values are estimated by using a neural network in-water algorithm for further iteration. The final output values for chl, ism, and cdom are generated via an empirical algorithm

B. Theoretical Description

(1) Methodology and Logic flow

1-1 Radiative transfer model

The satellite-observed reflectance, ρ_T, is modeled as follows.

$$\rho_T(\lambda) = \rho_M(\lambda) + \rho_A(\lambda) + \rho_{MA}(\lambda) + T(\lambda)\rho_G(\lambda) + t(\lambda)\rho_{WC}(\lambda) + t(\lambda)\rho_W(\lambda) \qquad (1)$$

where λ is wavelength, ρ_M is reflectance due to gas molecules, ρ_A is aerosol reflectance, ρ_{MA} is reflectance due to the interaction between molecules and aerosol particles, ρ_G is the reflectance resulting from the specular reflection of direct sun light, ρ_{WC} is the reflectance resulting from the whitecap, ρ_W is reflectance of the ocean, T is the direct transmittance of the atmosphere, and t is the diffuse transmittance of the atmosphere.

The purpose of atmospheric correction is to retrieve ρ_W in the equation above where ρ_A+ρ_{MA} and t are estimated by the satellite data with a help of aerosol lookup tables while ρ_M is calculated by a Rayleigh lookup table.

1-2 Aerosol models

We obtain the aerosol reflectance for 678nm and 865nm bands including the interaction part as follows,

$$\rho_A(\lambda) + \rho_{MA}(\lambda) = \rho_T(\lambda) - \rho_M(\lambda) - T(\lambda)\rho_G(\lambda) - t(\lambda)\rho_{WC}(\lambda) - t(\lambda)\rho_W(\lambda) \qquad (2)$$

We need to estimate ρ_A+ρ_{MA} for band 1 to 12 and 14 but it is not straight forward since the spectral relation of ρ_A+ρ_{MA} over the whole visible and near IR region is dependent on θ_0, θ, the satellite zenith angle, and $\Delta\phi$, the relative azimuth angle between the sun and the satellite, in addition to the type and optical thickness of aerosol. Similar to the method proposed by Gordon and Wang (1994), we introduce the tables that store the relation between the aerosol reflectance ρ_A+ρ_{MA} and aerosol optical thickness τ_A for each band and use them to determine the magnitude of ρ_A+ρ_{MA} in the shorter wavelengths bands based on the estimated spectral ratio of aerosol reflectance ε between two NIR bands. Since the relation between $\rho_A+\rho_{MA}$ and τ_A is dependent on aerosol type, GLI algorithm has the following nine candidate aerosol models:

- Tropospheric aerosol with R.H. of 70% (Model 1)
- Oceanic1600 aerosol with R.H. of 70% (Model 2)
- Oceanic800 aerosol with R.H. of 70% (Model 3)
- Oceanic400 aerosol with R.H. of 70% (Model 4)
- Oceanic200 aerosol with R.H. of 60 and 73% (Models 5 and 6)
- Oceanic100 aerosol with R.H. of 70% (Model 7)
- Oceanic50 aerosol with R.H. of 70 and 83% (Model 8 and 9)

The definition of these models are based on Shettle and Fenn (1979). The "Oceanic1600 type" consists of 99.9375% (one 1600th) of tropospheric and 0.0625% of oceanic aerosols, in terms of number of particles. RH means the assumed relative humidity. Other models through Model 9 are defined similarly.

1-3 Lookup tables

The following lookup tables were prepared beforehand to speed up processing of atmospheric correction.

- ρ_M table that gives $\rho_M(\lambda)$ for the given θ_0, θ, and $\Delta\phi$.
- "$\rho_A+\rho_{MA} \rightarrow \tau_A$" table that contains coefficients a_0, a_1, a_2, a_3 and a_4 in the equation,

$$\tau_A(\lambda) = a_0 + a_1 \cdot X(\lambda) + a_2 \cdot X(\lambda)^2 + a_3 \cdot X(\lambda)^3 + a_4 \cdot X(\lambda)^4 \quad (3)$$
$$X(\lambda) = \rho_A(\lambda) + \rho_{MA}(\lambda)$$

for all (θ_0, θ, $\Delta\phi$), aerosol types and atmospheric correction bands such as 678nm (ch13) and 865nm (ch19, denoted as 865A band).

- "$\tau_A \rightarrow \rho_A+\rho_{MA}$" table that contains coefficients a_0, a_1, a_2, a_3 and a_4 in the equation,

$$\rho_A(\lambda) + \rho_{MA}(\lambda) = a_0 + a_1 \cdot \tau_A(\lambda) + a_2 \cdot \tau_A(\lambda)^2 + a_3 \cdot \tau_A(\lambda)^3 + a_4 \cdot \tau_A(\lambda)^4 \quad (4)$$

for all (θ_0, θ, $\Delta\phi$), aerosol types and channels except atmospheric correction bands.

The entries for these tables were all generated by rstar5b code developed by T. Nakajima and his group.

1-3 consideration with absorptive aerosol

The standard GLI atmospheric correction algorithm (ver.1.5) has good performance, but it sometimes doesn't work well in East Asian region, when ocean is covered with absorptive aerosol like a forest fire smoke or anthropogenic black carbon. Hence, we added the following scheme for version 2 atmospheric correction.

We first define magnitude of aerosol absorption (aalb) as

$$aalb(\lambda) = \frac{[\rho_A(\lambda) + \rho_{MA}(\lambda)]}{\rho_A(\lambda) + \rho_{MA}(\lambda)} \quad (5)$$

where $\rho_A(\lambda)+\rho_{MA}(\lambda)$ is calculated from selected model based on the NIR bands.

We obtain the aalb at 380nm from $[\rho_A(380)+\rho_{MA}(380)]$ and $\rho_A(\tilde{380})+\rho_{MA}(\tilde{380})$. $[\rho_A(\tilde{380})+\rho_{MA}(380)]$ is calculated from eq.(2) by estimating water reflectance. When the absorption is significantly large, the $[\rho_A(\tilde{380})+\rho_{MA}(\tilde{380})]$ becomes much different from $\rho_A(\tilde{380})+\rho_{MA}(\tilde{380})$. In other words, the absorptive aerosol is detected from the difference, and is corrected by a spectral absorption model.

aalb for other bands is estimated by the following expression.

$$aalb(\lambda) = w(\lambda) \cdot aalb(380), \quad (6)$$

where w(λ) is weight of absorption. It is given empirically from scenes with an absorptive aerosol.

1-4 Atmospheric correction with iteration

We developed an iterative procedure that corrects atmospheric effect to avoid the black pixel assumption where near-infrared (NIR) water-leaving radiances are assumed to be zero or negligible (Siegel et al., 2000). As shown in Figure 3-1, the water reflectance at NIR bands are first estimated by using in-water model assuming initial values for chlorophyll a (chl) and inorganic suspended matter (ism) concentrations as well as absorption coefficient of colored dissolved organic matter (cdom). First atmospheric correction is executed, and new chl, ism and cdom are estimated by using neural network in-water algorithm. After the first atmospheric correction, new water-leaving reflectance is estimated from obtained chl, and the second stage atmospheric correction is conducted. This process is repeated until chl, ism and cdom estimates converge.

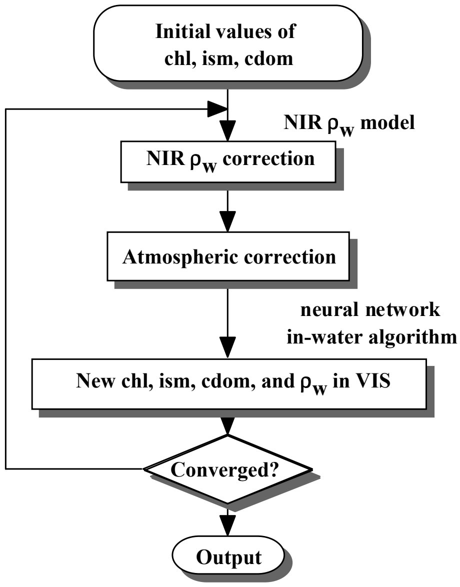

Fig. 3-1 A simplified flow diagram of the pixel-wise GLI atmospheric correction with iteration. In the diagram, NIR and VIS stand for the near-infrared and visible bands, respectively.

1-4-1. In-water model at near infrared region

The in-water model for NIR water-leaving radiance is defined as follows

$$[\rho_w(\lambda)]_N = 0.533\pi R(\lambda)/Q \quad (7)$$

by Lee et al. (1994) where λ is wavelength, and Q = 4.5 (Morel and Gentili, 1991). $[\rho_w(\lambda)]_N$ is normalized water-reflectance (Gordon, 1997) given by

$$[\rho_w(\lambda)]_N = \rho_w(\lambda)/t_0, \quad (8)$$

where t_0 is the transmittance between sun and ocean surface. R is the reflectance just below surface and is defined by Joseph (1950) as

$$R(\lambda) = \frac{\sqrt{1 + 2b_b(\lambda)/a(\lambda)} - 1}{\sqrt{1 + 2b_b(\lambda)/a(\lambda)} + 1} \quad (9)$$

where a and b_b is absorption and backward scattering coefficient, respectively. a(λ) and $b_b(\lambda)$ are defined by

$$a(\lambda) = a_w(\lambda) + a_c(\lambda, chl) + a_s(\lambda, ism) + a_y(\lambda), \quad (10)$$

and

$$b_b(\lambda) = b_{bw}(\lambda) + b_{bc}(\lambda, chl) + 2.7 \cdot b_{bs}(\lambda, ism) \quad (11)$$

where subscript w, c, s, y represents water, chlorophyll-a, inorganic suspended matter and yellow substance (cdom) respectively. Absorption coefficient values are given as follows.

$$a_w(678) = 0.42829,\quad a_w(865) = 4.6416 \tag{12}$$

by Pope and Fry (1997)

$$a_c(\lambda) = a_{cs}(\lambda) \cdot chl \tag{13}$$

where chl is chlorophyll a concentration in mg/m^3

$$a_{cs}(678) = 0.01968,\quad a_{cs}(865) = 0 \qquad \text{by Kishino (personal comm.)} \tag{14}$$

$$a_y(\lambda) = a_y(440) \cdot \exp\{-0.014 \cdot (\lambda - 440)\} \qquad \text{by Bricaud et al. (1981)} \tag{15}$$

The back scattering coefficients are given as follows:

$$b_{bw}(\lambda) = 0.5 \times 0.00288 \cdot \left(\frac{\lambda}{550}\right)^{-4.32} \qquad \text{by Morel (1974)} \tag{16}$$

$$b_{bc}(\lambda) = 0.081 \cdot b_c(\lambda) \qquad \text{by Oishi et al. (2002)} \tag{17}$$

$$b_c(\lambda) = 0.27.chl^{0.698} . \left(\frac{\lambda}{550}\right)^{-0.2933} \qquad \text{by Kishino (personal comm..)} \tag{18}$$

$$b_{bs}(\lambda) = b_s(\lambda) \cdot 0.01478 \qquad \text{by Babin and Doerffer (1996)} \tag{19}$$

$$b_s(\lambda) = 0.125 \cdot ism \cdot \left(\frac{\lambda}{550}\right)^{-0.812} \qquad \text{by Kronfeld (1988)} \tag{20}$$

3-2. Neural network-based in-water algorithm

A neural network is used for the iteration process to derive estimates of the chlorophyll-a concentration (chl), inorganic suspended solid concentration (ism) and absorption coefficient of colored dissolved organic matter (cdom) at 440nm (Tanaka et al., 1998)[11]. The inputs for the neural net are the normalized water-leaving radiances at 412, 443, 460, 520, and 545 nm bands. These bands are chosen because they have high saturation radiances.

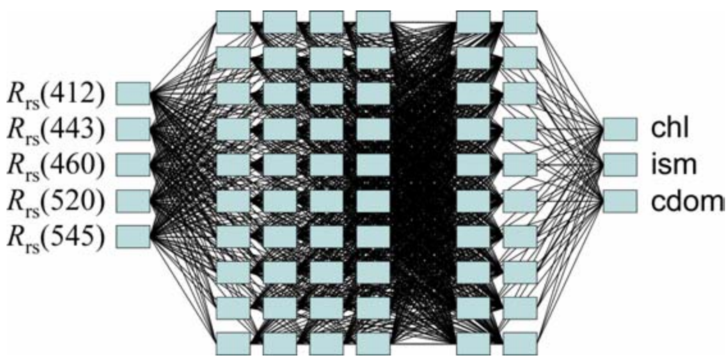

Figure 3-2 Neural network-based in-water algorithm

3-3. Alternative bands

Due to saturation problems of the GLI nominal band16 (749nm) and band18 (865nm) even in non-cloudy ocean areas, GLI band13 (678nm) and band19 (865nm), were used for atmospheric correction. An iteration scheme is needed since these bands may be influenced by upward radiance from the sea. These near-infrared (NIR) water-leaving radiance should be corrected before atmospheric correction by using specific in-water model.

(2) Physical and Mathematical aspects of the algorithm

This algorithm is originated from the OCTS atmospheric correction algorithm. An extension of the algorithm was made to improve the processing accuracies by taking use of many additional and new GLI bands. The OCTS algorithm, in turn, was initially developed based on an atmospheric correction method used to handle SeaWiFS data (Gordon and Wang, 1994), in taking the following effects into consideration:

・Polarized Rayleigh scattering (including the multiple scattering)
・Aerosol scattering
・Aerosol absorption
・Scattering among aerosol particles and gas molecules
・Reflection of sky light from sea surface
・Absorption effect by ozone
・Transmittance along the path sun-to-sea surface-to-satellite
・Sun glint
・Influence of white cap
・Absorbing effect of water vapor
・Absorbing effects of carbon dioxide gas and others

Corrections of the light components due to Rayleigh scattering, aerosol scattering, aerosol transmittance etc. are made by using lookup tables prepared beforehand. In addition to the atmospheric pressure, ozone concentration, wind speed etc., the atmospheric correction requires also other kinds of analysis data made available by Meteorological Agency.

C. References

1. Research Report: On the development of a retrieval algorithm for ADEOS-II/GLI ocean color data – Chapter 3: An Algorithm for GLI Ocean Color Atmospheric Correction, FY1996.
2. Research Report: Advanced Earth Observing Satellite (ADEOS) OCTS Data Processing Algorithm Description Ver.2.0 (NASDA) – Chapter 8.6: OCTS Type Algorithm.
3. Babin M. and R. Doerffer (1996), Specifications for case II coastal water reference model., Algorithm Theoretical Basis Document for MERIS (ATBD 2.12), ESA-ESTEC, pp.61-73.
4. Bricaud, A.,A. Morel and L. Prieur(1981), Absorption by dissolved organic matter of the sea (yellow substance) in the UV and visible domains, Limnol. Oceanogr., Vol.26, No.1, pp.43-53.
5. Ding, K. Y., & Gordon, H. R. (1994). Atmospheric correction of ocean color sensors: Effects of the earth's curvature. Applied Optics, 33 (30), 7096-7106.
6. Fukushima, H. A. Higurashi, Y. Mitomi, T. Nakajima, T. Noguchi, T. Tanaka, and M. Toratani (1998): Correction of atmospheric effect on ADEOS/OCTS ocean color data: Algorithm description and evaluation of its performance, J. Oceanography, 54, 417-430.

7. Fukushima, H. and M. Toratani (1997): Asian dust aerosol: optical effect on satellite ocean color signal and a scheme of its correction. J. Geophys. Res., 102(D14), 17,119-17,130
8. Gordon, H.R.(1997),Atmospheric correction of ocean color imagery in the Earth Observation System era, J. Geophys. Res., 102 (D14), 17,081-17,106.
9. Gordon, H.R., and M. Wang.(1994), Retrieval of water-leaving radiance and aerosol optical thickness over the oceans with SeaWiFS: a preliminary algorithm, Appl. Opt., 33 (3), 443-452.
10. Joseph, J. (1950), Untersuchungen über ober- und unterlichtmessungen im Meere und über ihren zusammenhang mit durchsichtigkeitsmessungen, Deut. Hydorograph. Z., Vol.3, pp.324-335.
11. Kronfeld, U. (1988),Die optishen eignenschatten der ozea nischen shwebstoffe und ihre bedentung fur fernerkundung von phytoplankton., GKSS Forschungszentrum, D-2054 Geesthacht, Germany, p.153.
12. Lee, Z., K. Carder, S. Hawes, R. Steward, T. Peacock and C. Davis (1944), Model for the interpretation of hyperspectral remote-sensing reflectance, Applied Optics, Vol.33, pp.5721-5732.
13. Morel A. and B. Gentili (1991), Diffuse reflectance of oceanic waters: its dependence on sun angle as influenced by the molecular scattering contribution, Applied optics, 30, 4427-4438.
14. Morel, A. (1974), Optical properties of pure water and pure sea water, chapter 1 in Optical Aspects of Oceanography, edited by N. G. Jerrov and E.S. Nielsen, Academic Press, New York, 1-24.
15. Nakajima, T., M. Tanaka, M. Yamamoto, M. Shiobara, K. Arao, and Y. Nakanishi (1989), Aerosol optical characteristics in the yellow sand events observed in May, 1982 at Nagasaki - part II models, J. Meteor. Soc. Japan, 67, 279-291.
16. Oishi, T., Y. Takahashi, A. Tanaka, M. Kishino, and A. Tsuchiya (2002), Relation between the backwordas well as total scattering coefficients and the volume scattering functions by cultured phytoplankton. J. School Mar. Sci. Technol. Tokai Univ., Vol.53, pp.1-15 (in Japanese with English abstract).
17. Pope, R. M. and E. S. Fry (1997), Absorption spectrum (380-700) of pure water, II: Integrating cavity measurement, Applied Optics, Vol.36, pp.8710-8723.
18. Shettle, E.P., and R. W. Fenn. (1979), Models for the aerosols of the lower atmosphere and the effects of humidity variations on their optical properties, AFGL-TR-79-0214, 675, 94pp,.
19. Siegel D. A., M. Wang, S. Maritorena, and W. Robinson (2000): Atmospheric correction of satellite ocean color imagery: the black pixel assumption, Appl. Opt., 30, 21, 3582-3591.
20. Tanaka, A., T. Oishi, M. Kishino, and R. Doerffer (1998), “Application of the neural network to OCTS data”, Proc. Ocean Optics XIV, S. G. Ackleson and J. Campbell (eds.), Office of Naval Research, Washington, D.C..